

Second Order QCD Corrections to $\Gamma(t \rightarrow Wb)$

K.G. Chetyrkin^{a,†}, R. Harlander^a, T. Seidensticker^a,
and M. Steinhauser^b

*(a) Institut für Theoretische Teilchenphysik,
Universität Karlsruhe, D-76128 Karlsruhe, Germany*

*(b) Institut für Theoretische Physik,
Universität Bern, CH-3012 Bern, Switzerland*

Abstract

Corrections of $\mathcal{O}(\alpha_s^2)$ to the decay of the top quark into a W boson and a bottom quark are calculated. The method is based on an expansion of the top quark propagator for small external momentum, q , as compared to the top quark mass, M_t . The physical point $q^2 = M_t^2$ is reached through Padé approximations. The described method allows to take effects induced by a finite W boson mass into account. The numerical relevance of the result is discussed. Important cross-checks against recent results for the decay rate $b \rightarrow ul\bar{\nu}$ and the two-loop QED corrections to μ -decay are performed.

[†]Permanent address: Institute for Nuclear Research, Russian Academy of Sciences, 60th October Anniversary Prospect 7a, Moscow 117312, Russia.

1 Introduction

The top quark is the so far heaviest observed particle of the Standard Model of elementary particle physics. Its total width, Γ_t , is to a good approximation proportional to the third power of its mass and is much larger than Λ_{QCD} , the typical scale of non-perturbative effects in QCD. Therefore it is possible to treat the top quark almost as a free particle and to apply perturbative methods to evaluate the quantum corrections to its decay process [1].

In the minimal Standard Model the dominant decay mode of the top quark is the one into a bottom quark and a W boson. It is important to predict the corresponding decay width accurately in order to be sensitive to exotic processes, which may occur in supersymmetric models, for example.

The first order QCD corrections have been evaluated in analytical form some time ago [2] and amount to approximately -10% . The electroweak corrections are small [3] and turn out to be $\approx 2\%$ for a Higgs mass around 100 GeV (see, e.g., [4]).

The expected precision for measurements of Γ_t by a future e^+e^- machine like the Next-Linear-Collider (NLC) is of the same order of magnitude as the corrections of $\mathcal{O}(\alpha_s)$ [4]. This makes it desirable to control also the next-to-leading corrections induced by the strong interaction.

In fact, the QCD corrections of $\mathcal{O}(\alpha_s^2)$ have already been considered in [5]. This calculation was based on an expansion of the vertex diagrams in the quantities $1 - M_b^2/M_t^2$ and $1 - 3M_b^2/M_t^2$, respectively. Although this expansion parameter is not small at all, the approach led to reliable results after including many terms into the analysis, choosing proper variables, and carefully investigating potentially large contributions.

The aim of this paper is, on the one hand, to have an independent check of the results of [5], using a rather complementary method. On the other hand, our approach will allow us to additionally account for a finite M_W boson mass.

The method presented in this paper is as follows. In contrast to [5] we compute propagator-type diagrams contributing to the top quark selfenergy with external momentum q in terms of an expansion around $q^2/M_t^2 = 0$. Some sample diagrams are pictured in Fig. 1. The imaginary part combined with the wave function renormalization of the top quark and evaluated at the physical point $q^2 = M_t^2$ directly leads to the decay rate. It arises from cuts where the W boson, the bottom quark and, at higher orders, also gluons and other light quarks are involved. The limit $q^2 \rightarrow M_t^2$ is taken after performing a Padé approximation. The results for $M_W = 0$ will be shown to be in perfect agreement with the ones of [5] which justifies both the method of [5] and the one of the present paper. The subleading terms in M_W^2 turn out to be numerically small.

The calculation once again demonstrates the power of expansion techniques and their computer implementations in multi-loop calculations. The analyticity properties of the approximated function guarantee reasonable convergence to the exact result, especially if

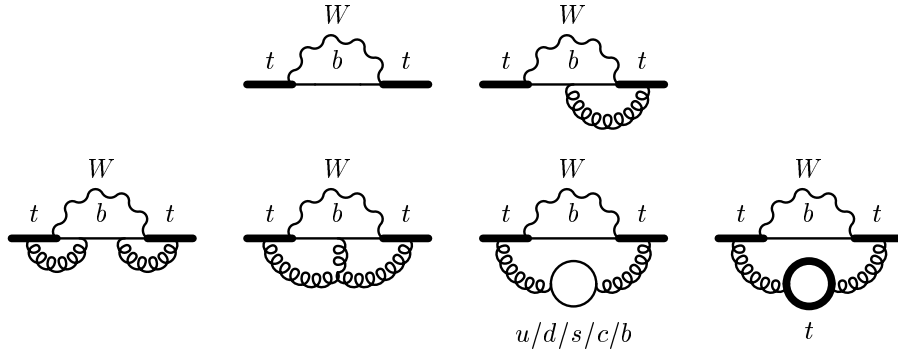


Figure 1: Sample diagrams for the top quark self energy.

the obtained series is further subject to advanced methods like Padé approximation.

The paper is organized as follows: In Section 2 the method is described. In Section 3, the results obtained at $\mathcal{O}(\alpha_s)$ are discussed in more detail. The comparison with the analytical result demonstrates the reliability of our method. Section 4 deals with the computation of the second order QCD corrections where also the effects of a finite W boson mass are taken into account. Important cross-checks with recent results for $\Gamma(b \rightarrow ul\bar{\nu})$ and $\Gamma(\mu \rightarrow e\nu_\mu\bar{\nu}_e)$ are carried out in Section 4.5.

2 Method of the calculation

The exact evaluation of the Feynman diagrams contributing to $\Gamma(t \rightarrow Wb)$ at order α_s^2 is currently not available. However, it is promising to apply the methods of asymptotic expansion (see, e.g., [6] and references therein) in the limit

$$M_t^2 \gg q^2 \gg M_W^2 \gg M_b^2 = 0. \quad (1)$$

For the $\mathcal{O}(\alpha_s)$ corrections in the limit $M_W = 0$, a similar approach has already been used in [7]. There it was possible to resum the series at $q^2 = M_t^2$ which reproduces the analytical result. At $\mathcal{O}(\alpha_s^2)$, however, instead of an explicit resummation we will perform a Padé approximation in order to reach the physical point $q^2 = M_t^2$ [8, 9].

Before going into details, let us introduce the notation. The inverse quark propagator is denoted by

$$\left(S_F^0(q)\right)^{-1} = i \left(m_t^0 \left(1 - \Sigma_S^0 \right) - \not{q} \left(1 + \Sigma_V^0 \right) \right). \quad (2)$$

Both Σ_S^0 and Σ_V^0 are functions of the external momentum q and the bare mass m_t^0 of the top quark. In our case they further depend on the bare strong coupling constant α_s^0 and the W boson mass M_W , and are proportional to the Fermi coupling constant, G_F . S_F^0

will become finite after renormalizing the parameters $m_t^0 = Z_m^{OS} M_t$ and $\alpha_s^0 = Z_g^2 \alpha_s$, and taking into account the wave function renormalization:

$$S_F^{OS} = \frac{1}{Z_2^{OS}} S_F^0. \quad (3)$$

Z_m^{OS} , Z_2^{OS} and Z_g denote the renormalization constants. Z_m^{OS} and Z_2^{OS} will be taken in the on-shell scheme, whereas Z_g is in the $\overline{\text{MS}}$ scheme. Z_2^{OS} is defined by the condition

$$S_F^{OS}(q) \longrightarrow \frac{-i}{M_t - \not{q}} + \text{terms regular for } q^2 \rightarrow M_t^2. \quad (4)$$

In our approach we are actually dealing with two different masses for the top quark in intermediate steps: an “external” one (q^2) and an “internal” one (M_t^2). Applying the optical theorem, the decay rate of the top quark will therefore be written as

$$\Gamma(t \rightarrow Wb) = (2M_t \text{Im}[z S_V^{OS} - S_S^{OS}]) \Big|_{z=1}, \quad (5)$$

where

$$\begin{aligned} S_S^{OS} &= Z_2^{OS} Z_m^{OS} (1 - \Sigma_S^0), \\ S_V^{OS} &= Z_2^{OS} (1 + \Sigma_V^0) \end{aligned} \quad (6)$$

are functions of the variable

$$z = \frac{q^2}{M_t^2}. \quad (7)$$

All relevant diagrams will be calculated in terms of expansions around $z = 0$, and the limit $z \rightarrow 1$ will be applied only in the very end. Therefore, while Z_m^{OS} can be taken at $z = 1$, we also need to express Z_2^{OS} in terms of an expansion around $z = 0$. This is most conveniently done by translating condition (4) into

$$Z_2^{OS} = \left[1 + \Sigma_V^0 + 2 \frac{d}{dz} (Z_m^{OS} \Sigma_S^0 - \Sigma_V^0) \right]^{-1}. \quad (8)$$

From (5) and (6) it is clear that for our purpose it suffices to know only the pure QCD corrections of Z_2^{OS} and Z_m^{OS} up to $\mathcal{O}(\alpha_s^2)$. For $z = 1$ these quantities were computed up to this order in [10] and [11], respectively.

Note that in a calculation where the quantities are evaluated on-shell, i.e. at $q^2 = M_t^2$, infra-red singularities appear in intermediate steps. In contrast, in Eq. (6) all functions on the r.h.s. are defined through the expansion for $z \rightarrow 0$ and thus are infra-red safe.

At this point a comment on the extraction of the values for $z = 1$ is in order. Actually Eqs. (5) and (8) are not unique as it is possible to derive slightly different equations for Z_2^{OS} and $\Gamma(t \rightarrow Wb)$, which differ by relative factors of z . In the limit $z \rightarrow 1$ all of them

are equivalent. The results we obtained by using two more variants of Eqs. (5) and (8) are consistent with the ones which will be discussed below. We decided to use the formulae shown above because the $\mathcal{O}(\alpha_s)$ corrections are recovered with the highest accuracy.

In order to obtain reliable results it is necessary to evaluate as many terms as possible in the expansion parameter z . The exact resummation of the series in z seems to be excluded. Instead, we apply a Padé approximation which means that we reexpress the resulting polynomial in terms of a rational function:

$$[m/n](z) = \frac{a_0 + a_1 z + \dots + a_m z^m}{1 + b_1 z + \dots + b_n z^n}. \quad (9)$$

Its Taylor series is required to coincide with the original polynomial up to the order $m+n$. For later convenience we define the short hand notation $[m/n] \equiv [m/n](1)$. The stability of the Padé approximants upon variation of m and n will indicate the uncertainty of the approximation (see below).

In addition, it may be promising to apply a conformal mapping [8]

$$z = \frac{4\omega}{(1+\omega)^2} \quad (10)$$

and to perform the Padé approximation in the variable ω . The complex z -plane is mapped into the interior of the unit circle in the ω -plane, and the relevant point $z = 1$ goes to $\omega = 1$. This conformal mapping is motivated by the observation that the application of a Padé approximation relies heavily on analytic properties. The function on the r.h.s. of Eq. (5) (without the limit $z \rightarrow 1$) will develop a branch cut along the real z -axis starting from $z = 1$. This branch cut is mapped through Eq. (10) onto the unit circle. Thus by applying Eq. (10) we enlarge the range of convergence for the terms we got in the limit $z \rightarrow 0$.

Since both methods described above appear to be rather natural, any of them will be used to derive an estimate on the exact result. For convenience, let us denote the results obtained through Padé approximation in the variable z by “ z -Padés”, the ones where the Padé approximation is performed in ω by “ ω -Padés”. The central values and the estimated uncertainty will be extracted from Padé results $[m/n]$ with $m+n$ not too small and $|m-n| \leq 2$. The central value is obtained by averaging the Padé results and the uncertainty is given by the maximum deviation from the central value. The error estimation is therefore rather conservative.

Some Padé approximants develop poles inside the unit circle ($|z| \leq 1$ and $|\omega| \leq 1$, respectively). In general we will discard such results in the following. In some cases, however, the pole coincides with a zero of the numerator up to several digits accuracy, and these Padé approximations will be taken into account for the estimation of the actual results. To be precise: in addition to the Padé results without any poles inside the unit circle, we will use the ones where the poles are accompanied by zeros within a circle of radius 0.01, and the distance between the pole and the physically relevant point $q^2/M_t^2 = 1$ is larger than 0.1.

Concerning the dependence on the strong gauge parameter ξ in Eq. (5), it only drops out after summing infinitely many terms in the expansion around $z = 0$ and setting $z = 1$. Since we are only dealing with a limited number of terms, our approximate results will still depend on the choice of ξ even after taking $z \rightarrow 1$. It is clear that with extreme values of ξ almost any number could be produced. Thus the question arises which value of ξ should be assumed in order to arrive at a reliable prediction for $\Gamma(t \rightarrow Wb)$.

At $\mathcal{O}(\alpha_s)$ the whole calculation can be performed for arbitrary gauge parameter without any difficulties. This allows for a detailed study of the residual ξ dependence. At $\mathcal{O}(\alpha_s^2)$ only the first few terms could be evaluated for general ξ which does not allow for extensive studies. In order to arrive at a reasonable number of terms in the expansion around $z = 0$ it is necessary to set ξ to some definite value from the very beginning. The behaviour of the diagrams at $\mathcal{O}(\alpha_s)$ will serve as an indication for the optimal choice of this value in the analysis at $\mathcal{O}(\alpha_s^2)$.

Concerning the electroweak gauge parameter ξ_W , all results that will be quoted in the following have been obtained in unitary gauge, where the W propagator is given by

$$D_W(p) = \frac{-i}{M_W^2 - p^2} \left(-g_{\mu\nu} + \frac{p_\mu p_\nu}{M_W^2} \right). \quad (11)$$

Nevertheless, the leading terms in M_W have also been computed in an arbitrary covariant gauge. They are obtained by replacing the W boson by a Goldstone boson with the propagator simply given by

$$D_\Phi(p) = \frac{-i}{\xi_W M_W^2 - p^2} \xrightarrow{M_W \rightarrow 0} \frac{i}{p^2}. \quad (12)$$

The independence of ξ_W is then manifest already at this point.

3 First order QCD corrections

In this section we will investigate the $\mathcal{O}(\alpha_s)$ corrections and compare the exact result [2] to the approximation obtained by the method described above.

It is convenient to decompose the decay rate of the top quark into a W boson and a bottom quark in the following way:

$$\Gamma(t \rightarrow bW) = \Gamma_0 \left[A^{(0)} + \frac{\alpha_s}{\pi} C_F A^{(1)} + \left(\frac{\alpha_s}{\pi} \right)^2 A^{(2)} + \dots \right], \quad (13)$$

where $\Gamma_0 = G_F M_t^3 |V_{tb}|^2 / (8\pi\sqrt{2})$, $A^{(0)} = 1 - 3M_W^4/M_t^4 + 2M_W^6/M_t^6$, $C_F = 4/3$, and V_{tb} is the CKM matrix element for $t \rightarrow b$ transitions. The running coupling α_s is defined with six active flavours.

The one-loop correction is known in analytical form since quite some time [2]. Expanded in terms of M_W/M_t it reads:

$$A^{(1)} = \frac{5}{4} - \frac{\pi^2}{3} + \frac{3}{2} \frac{M_W^2}{M_t^2} + \frac{M_W^4}{M_t^4} \left(-6 + \pi^2 - \frac{3}{2} \ln \frac{M_t^2}{M_W^2} \right) + \frac{M_W^6}{M_t^6} \left(\frac{46}{9} - \frac{2}{3} \pi^2 + \frac{2}{3} \ln \frac{M_t^2}{M_W^2} \right) + \mathcal{O} \left(\frac{M_W^8}{M_t^8} \right). \quad (14)$$

The approximation $M_W = 0$ induces an error of roughly 22%. This reduces to approximately 4% if the quadratic mass corrections are included and is completely negligible if all the terms displayed in Eq. (14) are taken into account.

For clarity, let us apply our method to these lowest order terms and see how the results compare to $A^{(0)}$ and $A^{(1)}$ above. While $A^{(0)}$ is reproduced exactly, the imaginary part of the small-momentum expansion for the two-loop ($\mathcal{O}(\alpha_s)$) diagrams (an example is shown in Fig. 1) reads:

$$\begin{aligned} A_{exp}^{(1)} = & -\frac{19}{12} - \frac{29}{144} z - \frac{23}{240} z^2 - \frac{61}{1200} z^3 - \frac{151}{5040} z^4 - \frac{449}{23520} z^5 - \frac{13}{1008} z^6 \\ & - \frac{827}{90720} z^7 - \frac{529}{79200} z^8 \\ & + \xi \left(\frac{5}{12} - \frac{7}{48} z - \frac{1}{16} z^2 - \frac{3}{80} z^3 - \frac{43}{1680} z^4 - \frac{3}{160} z^5 - \frac{29}{2016} z^6 \right. \\ & \quad \left. - \frac{23}{2016} z^7 - \frac{49}{5280} z^8 \right) \\ & + \frac{M_W^2}{M_t^2 z} \left[\frac{3}{2} + \frac{1}{18} z - \frac{1}{72} z^2 - \frac{7}{600} z^3 - \frac{7}{900} z^4 - \frac{23}{4410} z^5 - \frac{17}{4704} z^6 \right. \\ & \quad \left. - \frac{47}{18144} z^7 - \frac{31}{16200} z^8 \right] \\ & + \frac{M_W^4}{M_t^4 z^2} \left[\frac{1}{4} + \frac{13}{3} z - \frac{383}{720} z^2 - \frac{79}{720} z^3 - \frac{313}{8400} z^4 - \frac{403}{25200} z^5 - \frac{557}{70560} z^6 \right. \\ & \quad \left. - \frac{151}{35280} z^7 - \frac{2477}{997920} z^8 \right] \\ & + \xi \left(\frac{5}{4} - \frac{5}{2} z + \frac{37}{80} z^2 + \frac{3}{16} z^3 + \frac{61}{560} z^4 + \frac{41}{560} z^5 + \frac{179}{3360} z^6 \right. \\ & \quad \left. + \frac{137}{3360} z^7 + \frac{239}{7392} z^8 \right) \\ & + l_{tW} \left(\frac{3}{4} - \frac{9}{4} z - \frac{3}{4} \xi + \frac{3}{4} z \xi \right) + \mathcal{O} \left(\frac{M_W^6}{M_t^6} \right), \quad (15) \end{aligned}$$

with $l_{tW} = \ln M_t^2/M_W^2$. (The coefficient of z^n will be called the “ n^{th} moment” in the following.) Note that the factors $1/z$ and $1/z^2$ in front of the quadratic and quartic terms in M_W are irrelevant for the subsequent Padé procedure.

The procedure described above is applied to each coefficient of M_W^2/M_t^2 separately. As already noted, $A_{exp}^{(1)}$ still depends on the QCD gauge parameter, ξ , appearing in the gluon propagator $i(-g^{\mu\nu} + \xi q^\mu q^\nu/q^2)/(q^2 + i\epsilon)$. Thus also the Padé approximations $[m/n]$ will show a dependence on ξ . It is clear that for large absolute values of ξ the quantities $[m/n]$ get dominated by them and any predictive power is lost. In Table 1 several z -Padés are evaluated for the leading order coefficient ($M_W = 0$). The gauge parameter is varied from $\xi = -2$ to $\xi = +2$. Padé results which develop poles for $|z| \leq 1$ are in general represented by a dash. However, if an approximate cancellation with a zero from the numerator takes place (see the discussion above), they are marked by a star (\star). The exact result is reproduced with a fairly high accuracy for almost all values of ξ under consideration. Nevertheless, the value for $\xi = 0$ is closest to the exact result, and the variation of the Padé approximants appears to be very small for this particular choice of ξ . Based on this observation, we decide to perform the three-loop analysis by setting $\xi = 0$. This has the additional advantage that the evaluation of the Feynman diagrams is much simpler than for non-zero values of ξ .

input	P.A.	$\xi = -2$	$\xi = -1$	$\xi = -1/2$	$\xi = 0$	$\xi = 1/2$	$\xi = 1$	$\xi = 2$
6	$[3/2]$	-2.111	—	-2.058	-2.023	-1.990	-1.957	-1.893
6	$[2/3]$	-2.112	-2.052	-2.058	-2.023	-1.990	-1.963	-1.887
7	$[4/2]$	-2.121	—	-2.058	-2.027	-1.999	-1.972	-1.919
7	$[3/3]$	-2.120	—	-2.058	(\star) -2.025	-2.008	-1.980	-1.928
7	$[2/4]$	-2.126	—	-2.058	-2.027	-2.000	-1.979	-1.912
8	$[4/3]$	-2.117	—	—	-2.033	-2.011	-1.990	-1.949
8	$[3/4]$	-2.117	-1.694	-2.058	-2.033	-2.011	-1.993	-1.948
9	$[5/3]$	-2.112	-2.063	(\star) -2.059	-2.034	-2.016	-1.998	-1.963
9	$[4/4]$	-2.105	-2.061	(\star) -2.059	-2.034	-2.040	-2.001	-1.967
9	$[3/5]$	-2.114	-2.064	(\star) -2.059	-2.034	-2.016	-2.001	-1.961
exact:		-2.040						

Table 1: z -Padés for $A^{(1)}|_{M_W=0}$ for different values of ξ . The first column indicates the number of terms in z from (15) that were used as input.

Let us now discuss the sub-leading terms in M_W^2 . Table 2 lists several Padé approximations for the coefficients of $(M_W^2/M_t^2)^n$ ($n = 0, 1, 2$) in the case of $A^{(1)}$. ξ has been set to zero, as it is suggested by the discussion above. For each coefficient, the Padé approximations have been performed in the variable z as well as in the variable ω . The z - and ω -Padés are indicated by a z and an ω , respectively, in the second line of Table 2. This notation will be used throughout the paper. The z -Padés for the values of the $(M_W^2/M_t^2)^0$ -term coincide with those for $\xi = 0$ of Table 1, of course. Concerning the power-suppressed terms, again the higher order Padé approximants agree with the exact results to an impressive accuracy. The logarithm of Eq. (14) is reproduced exactly after taking into account the first two terms in the expansion (15) and setting $z = 1$.

Also for the power-suppressed terms an analysis concerning the ξ dependence has been

		M_W^0		M_W^2		M_W^4	
input	P.A.	z	ω	z	ω	z	ω
6	[3/2]	-2.023	-2.022	1.506	1.508	3.875	—
6	[2/3]	-2.023	-2.051	—	1.548	3.878	—
7	[4/2]	-2.027	(*) - 2.009	(*) 1.507	(*) 1.518	3.871	—
7	[3/3]	(*) - 2.025	-2.035	—	1.501	3.872	—
7	[2/4]	-2.027	-2.040	—	1.507	3.874	—
8	[4/3]	-2.033	-2.035	1.502	1.502	3.870	—
8	[3/4]	-2.033	-2.035	—	1.502	3.870	—
9	[5/3]	-2.034	-2.039	1.502	1.500	3.870	—
9	[4/4]	-2.034	(*) - 2.035	1.502	(*) 1.501	3.870	—
9	[3/5]	-2.034	-2.037	1.502	1.499	3.870	—
exact:		-2.040		1.500		3.870	

Table 2: Padé approximations for the power-suppressed terms of $A^{(1)}$, computed for $\xi = 0$.

performed. While the quadratic terms in M_W do not depend on ξ at all (see Eq. (15)), the results for the terms of order M_W^4/M_t^4 become significantly worse once ξ is different from zero. This also supports the choice of Feynman gauge at three loops.

Taking only those results of Table 2 into account where eight or more input terms enter we may finally deduce our approximation for the $\mathcal{O}(\alpha_s)$ corrections to the decay rate (we adopt the notation $-2.035(4) \equiv -2.035 \pm 0.004$, etc.):

$$A^{(1)} = -2.035(4) + 1.501(2) \frac{M_W^2}{M_t^2} + \frac{M_W^4}{M_t^4} \left(3.8700(5) - \frac{3}{2} \ln \frac{M_t^2}{M_W^2} \right) + \dots \quad (16)$$

The agreement of Eq. (16) with the exact results quoted in the last line of Table 2 obviously supports the underlying method.

In the three-loop case we could obtain the small-momentum expansion up to z^7 for $M_W = 0$ and up to z^6 for the coefficients of M_W^2/M_t^2 and the M_W^4/M_t^4 . Therefore, the final number at three-loop level will be based on Padés built out of seven and eight moments for the leading term, and six and seven moments for the sub-leading terms in M_W . At $\mathcal{O}(\alpha_s)$ this reduced number of input terms changes the result from the one in (16) to

$$A^{(1)} = -2.03(2) + 1.51(4) \frac{M_W^2}{M_t^2} + \frac{M_W^4}{M_t^4} \left(3.874(4) - \frac{3}{2} \ln \frac{M_t^2}{M_W^2} \right) + \dots \quad (17)$$

which is a bit worse than (16), but still sufficiently accurate. This suggests that the number of available moments at order α_s^2 should be sufficient to arrive at a reasonable estimate.

4 Second order QCD corrections

Let us use the experience gained in the previous section to obtain predictions for $\Gamma(t \rightarrow Wb)$ at order α_s^2 .

4.1 General remarks

It is convenient to decompose the decay rate according to the colour structure:

$$A^{(2)} = C_F^2 A_A^{(2)} + C_A C_F A_{NA}^{(2)} + C_F T n_l A_l^{(2)} + C_F T A_F^{(2)}, \quad (18)$$

where in QCD the colour factors are given by $C_F = 4/3$, $C_A = 3$, and $T = 1/2$. n_l is the number of massless quark flavours and will be set to $n_l = 5$ in the end. $A_A^{(2)}$ corresponds to the abelian part already present in QED, $A_{NA}^{(2)}$ represents the non-abelian contribution, and $A_l^{(2)}$ and $A_F^{(2)}$ denote the corrections involving a second fermion loop with massless and massive quarks, respectively. In Fig. 1 a representative diagram for each function is pictured. The expansion in terms of M_W^2/M_t^2 of the individual contributions to $A^{(2)}$ will be written as

$$A_i^{(2)} = A_i^{(2)}|_{M_W=0} + \frac{M_W^2}{M_t^2} A_i^{(2)}|_{M_W^2} + \frac{M_W^4}{M_t^4} A_i^{(2)}|_{M_W^4} + \dots, \quad (19)$$

with $i = A, NA, l$ and F . Note that $A_l^{(2)}|_{M_W=0}$ is known analytically [12] and serves as a welcome check for our method.

Whereas at $\mathcal{O}(\alpha_s)$ the 't Hooft mass μ^2 drops out (see Eq. (15)), it does appear at $\mathcal{O}(\alpha_s^2)$. We adopted the convention $\mu^2 = M_t^2$ throughout the paper.

There are 60 three-loop diagrams that contribute to $\Gamma(t \rightarrow Wb)$. The practical computation is done with the help of the package **GEFICOM** [13]. It uses **QGRAF** [14] for the generation of the diagrams and **EXP** [15] for the application of the hard mass procedure. For more details we refer to a recent review concerned with the automatic computation of Feynman diagrams [6]. The application of the methods of asymptotic expansion according to Eq. (1) reduces the practical computation either to massless three-loop propagator-type diagrams or to products of one- and two-loop integrals. In the latter case either vacuum graphs or again massless two-point functions appear. The integrals have been performed with the help of the packages **MINCER** [16] and **MATAD** [17] based on the symbolic manipulation language **FORM** [18]. The results for Σ_S^0 and Σ_V^0 defined in Eqs. (5) and (8) at three loops are quite lengthy and therefore not listed here. They can be obtained from the authors upon request.

4.2 The limit $M_W = 0$

This section is concerned with the second order QCD corrections where the mass of the W boson is neglected. In this limit a comparison with [5] can be performed. The M_W -

suppressed corrections will be discussed in the subsequent section. As already noted, $A_{A,exp}^{(2)}(z)$ and $A_{NA,exp}^{(2)}(z)$ were computed up to z^7 in the case of a massless W boson in Feynman gauge which corresponds to eight input terms for the Padé approximations.

The fermionic pieces, $A_{l,exp}^{(2)}$ and $A_{F,exp}^{(2)}$, do not depend on the QCD gauge parameter and are of simpler structure than $A_{A,exp}^{(2)}$ and $A_{NA,exp}^{(2)}$. For the light-fermion contribution we thus could evaluate nine terms in the expansion around $z = 0$ for the leading term in M_W .

In Table 3 the results are displayed. The z -Padés for $A_F^{(2)}$ converge very quickly whereas most of the ω -Padés develop poles for $|\omega| \leq 1$. As a result we infer

$$A_F^{(2)} \Big|_{M_W=0} = -0.06360(1), \quad (20)$$

which coincides with the one quoted in [5]. Note, however, that the magnitude of $A_F^{(2)}$ is rather small.

		$A_l^{(2)}$		$A_F^{(2)}$		$A_A^{(2)}$		$A_{NA}^{(2)}$	
input	P.A.	z	ω	z	ω	z	ω	z	ω
6	[3/2]	2.600	2.889	-0.06359	—	2.971	—	-7.637	-8.238
6	[2/3]	2.600	2.994	-0.06359	-0.06464	2.972	—	-7.639	-8.400
7	[4/2]	2.633	2.920	-0.06360	—	3.041	3.818	-7.710	-8.212
7	[3/3]	(*) 2.592	2.926	-0.06360	—	3.140	—	-7.781	-8.218
7	[2/4]	2.636	2.956	-0.06359	—	3.046	—	-7.719	-8.306
8	[4/3]	2.695	(*) 2.907	-0.06360	—	3.146	—	-7.820	(*) -8.232
8	[3/4]	2.696	2.832	-0.06360	—	3.146	—	-7.820	-8.254
9	[5/3]	2.708	2.881						
9	[4/4]	2.707	2.892						
9	[3/5]	2.708	2.902						
exact:		2.859							

Table 3: Padé results at $\mathcal{O}(\alpha_s^2)$ for $M_W = 0$.

$A_l^{(2)}$ behaves similar to the $\mathcal{O}(\alpha_s)$ corrections. As expected, the more terms of the expansion in z are included, the better agreement with the exact result is observed. Furthermore, both z -Padés and ω -Padés lead to compatible numerical values from which, including the seventh and eighth moment (“input 8” and “input 9” in Table 3), the following result is deduced:

$$A_l^{(2)} \Big|_{M_W=0} = 2.8(1). \quad (21)$$

The error is around 4% and thus roughly as large as the one in [5], where the result reads 2.85(7). Using only the sixth and seventh moment one ends up with

$$A_l^{(2)} \Big|_{M_W=0} = 2.8(2), \quad (22)$$

where the error is 7%. The result of Eqs. (21) and (22) can also be compared with the exact number [12] which reads 2.859...

Let us now turn to the abelian and non-abelian parts. Like in the one-loop case, the expansion in z is gauge dependent for these contributions. Motivated by the observations of Section 3, the analysis will be performed by setting $\xi = 0$ from the very beginning. For non-zero values of ξ some lower-order Padé approximants will be presented at the end of this section.

As compared to the fermionic contributions, the spread among the z -Padés and ω -Padés is significantly larger. Moreover, the numbers for the two approaches are less compatible with each other. Nevertheless, following the previously introduced strategy for the extraction of the central value and the error, we obtain

$$A_A^{(2)} \Big|_{M_W=0} = 3.2(6), \quad (23)$$

$$A_{NA}^{(2)} \Big|_{M_W=0} = -8.0(3). \quad (24)$$

The (fairly conservative) errors are larger than the ones of the results in [5], which read 3.5(2) and $-8.10(17)$, respectively. The numbers, however, are consistent.

At this point we have confirmed the results of [5] with a completely independent method. Our calculation can therefore serve as an important cross check.

Due to the complexity of the intermediate expressions it was impossible to evaluate eight terms in the expansion for small z using a general gauge parameter. In this case, we managed to compute the expansions for $A_A^{(2)}$ and $A_{NA}^{(2)}$ only up to terms of $\mathcal{O}(z^3)$. In Tables 4 and 5 the gauge parameter is varied between $\xi = -2$ and $\xi = +2$. For $A_A^{(2)}$ the error bars of Eq. (23) are conservative enough to cover even most of the values of Table 4. The stability of $A_{NA}^{(2)}$ against variations of ξ is also satisfactory, although many of the values of Table 5 are not compatible with (24). However, this could be traced to the low number of input terms in Table 5.

input	P.A.	$\xi = -2$	$\xi = -1$	$\xi = -1/2$	$\xi = 0$	$\xi = 1/2$	$\xi = 1$	$\xi = 2$
3	[2/0]	2.790	2.425	2.305	2.226	2.189	2.194	2.329
3	[1/1]	2.780	—	2.685	2.508	2.518	2.632	3.254
3	[0/2]	2.787	2.432	2.329	2.280	2.293	2.375	2.789
4	[3/0]	2.849	2.501	2.397	2.341	2.332	2.369	2.586
4	[2/1]	(*)2.624	3.268	2.810	2.713	2.725	2.816	3.201
4	[1/2]	(*)2.705	3.320	2.810	2.721	2.739	2.827	3.202
4	[0/3]	2.847	2.517	2.433	2.411	2.455	2.572	3.047

Table 4: ξ dependence of $A_A^{(2)}|_{M_W=0}$.

input	P.A.	$\xi = -2$	$\xi = -1$	$\xi = -1/2$	$\xi = 0$	$\xi = 1/2$	$\xi = 1$	$\xi = 2$
3	[2/0]	-7.894	-6.953	-6.571	-6.248	-5.984	-5.779	-5.547
3	[1/1]	-8.202	-7.455	-7.176	-6.954	-6.783	-6.655	-6.515
3	[0/2]	-8.078	-7.243	-6.924	-6.669	-6.476	-6.340	-6.219
4	[3/0]	-8.117	-7.262	-6.915	-6.623	-6.385	-6.202	-5.997
4	[2/1]	-8.335	-7.670	-7.417	-7.212	-7.051	-6.930	-6.802
4	[1/2]	-8.346	-7.690	-7.440	-7.236	-7.075	-6.956	-6.834
4	[0/3]	-8.241	-7.493	-7.209	-6.984	-6.813	-6.691	-6.580

Table 5: ξ dependence of $A_{NA}^{(2)}|_{M_W=0}$.

4.3 Subleading terms in M_W

Let us now turn to the power-suppressed terms of order $(M_W^2/M_t^2)^n$ ($n > 0$). Both for the $\mathcal{O}(M_W^2/M_t^2)$ and $\mathcal{O}(M_W^4/M_t^4)$ contribution seven terms in the expansion in z could be evaluated.

4.3.1 Quadratic terms in M_W

		$A_l^{(2)}$		$A_F^{(2)}$		$A_A^{(2)}$		$A_{NA}^{(2)}$	
input	P.A.	z	ω	z	ω	z	ω	z	ω
6	[3/2]	—	-1.016	0.09766	0.09769	$(*) - 2.721$	—	3.358	—
6	[2/3]	$(*) - 1.013$	-0.9459	0.09766	0.09769	-2.747	—	3.358	—
7	[4/2]	-0.9737	-0.9773	0.09766	0.09764	$(*) - 2.677$	-2.794	3.353	—
7	[3/3]	-0.9758	-0.9676	0.09766	—	$(*) - 2.677$	—	3.354	—
7	[2/4]	-0.9652	-1.122	0.09766	0.09764	-2.770	—	3.356	—

Table 6: Padé results for the $\mathcal{O}(\alpha_s^2)$ coefficients at $\mathcal{O}(M_W^2/M_t^2)$.

The resulting Padé values for the quadratic M_W terms are listed in Table 6. The light-fermion contribution is very stable and the maximal deviation from the central value amounts to roughly 10%. Like in the case $M_W = 0$, the Padé approximants for $A_F^{(2)}$ — both in ω and z — exhibit an impressive convergence.

For the abelian and non-abelian contribution most of the ω -Padés develop poles inside $|\omega| \leq 1$. In addition, while the z -Padés for $A_{NA}^{(2)}$ are very smooth, for $A_A^{(2)}$ there are only two of them without poles within $|z| \leq 1$. However, all the poles of the other z -Padés approximately cancel against zeros in the numerator. All relevant numbers are highly consistent.

Therefore, the numbers in Table 6 lead us to the following results:

$$\begin{aligned}
A_A^{(2)} \Big|_{M_W^2} &= -2.73(6), \\
A_{NA}^{(2)} \Big|_{M_W^2} &= 3.356(3), \\
A_l^{(2)} \Big|_{M_W^2} &= -1.0(1), \\
A_F^{(2)} \Big|_{M_W^2} &= 0.09766(3).
\end{aligned} \tag{25}$$

4.3.2 Quartic terms in M_W

In Table 7 the Padé approximations for the quartic terms in M_W are listed. The conformal mapping seems to spoil the convergence property here, as all ω -Padés develop poles within the unit circle. Moreover, in contrast to the constant and quadratic corrections, for the M_W^4 terms it turns out that variations of Eqs. (5) and (8) (see the discussion in Section 2) lead to results which lie outside the error interval obtained from the numbers of Table 7. So the final numbers for the M_W^4 terms should only be considered as estimates on their order of magnitude. They will be presented below, with an artificially increased error of about 50%.

		$A_l^{(2)}$		$A_F^{(2)}$		$A_A^{(2)}$		$A_{NA}^{(2)}$	
input	P.A.	z	ω	z	ω	z	ω	z	ω
6	[3/2]	-1.290	—	0.1474	—	—	—	2.364	—
6	[2/3]	-1.291	—	(*)0.1384	—	(*)4.606	—	2.448	—
7	[4/2]	(*) - 1.268	—	0.1479	—	(*)4.460	—	2.489	—
7	[3/3]	(*) - 1.278	—	0.1477	—	(*)4.461	—	2.459	—
7	[2/4]	-1.305	—	0.1489	—	—	—	2.460	—

Table 7: Padé results for the $\mathcal{O}(\alpha_s^2)$ coefficients at $\mathcal{O}(M_W^4/M_t^4)$.

While the leading two terms in M_W do not contain logarithms of M_W , the coefficients of M_W^4 develop linear logarithms of M_W^2/M_t^2 . For $A^{(1)}$ the coefficient of this logarithm is exactly reproduced by the first two terms in the Taylor expansion around $z = 0$ after setting $z = 1$; the higher order terms in z vanish (a similar behaviour for the logarithmic terms has already been observed in [19]). The phenomenon of a truncated series in z for this coefficient also appears for $A_{l,exp}^{(2)}$ and $A_{F,exp}^{(2)}$. According to the discussion above, this strongly suggests that the logarithms of M_W are exactly recovered after setting $z = 1$. While for $A_l^{(2)}$ one arrives at $7/4 \cdot \ln M_t^2/M_W^2$ for the term under consideration, it sums up to zero for $A_F^{(2)}$.

For the abelian and non-abelian parts, the series in z for the coefficients of the $M_W^4/M_t^4 \cdot \ln M_t^2/M_W^2$ term does not seem to be truncated, but the Padé analysis turns out to be very stable. It can be found in Table 8.

		$A_A^{(2)}$		$A_{NA}^{(2)}$	
input	P.A.	z	ω	z	ω
6	[3/2]	0.7811	—	−3.614	—
6	[2/3]	0.7829	—	−3.614	—
7	[4/2]	0.7334	—	−3.626	—
7	[3/3]	0.7747	—	−3.618	—
7	[2/4]	0.7594	—	−3.622	—

Table 8: Padé results for the coefficient of $M_W^4/M_t^4 \cdot \ln(M_W^2/M_t^2)$ for $A_A^{(2)}$ and $A_{NA}^{(2)}$.

Finally, the results for the quartic contributions in M_W^4 read:

$$\begin{aligned}
A_A^{(2)} \Big|_{M_W^4} &= 4.5(2.2) + 0.7(1) \ln \frac{M_t^2}{M_W^2}, \\
A_{NA}^{(2)} \Big|_{M_W^4} &= 2.4(1.2) - 3.62(1) \ln \frac{M_t^2}{M_W^2}, \\
A_t^{(2)} \Big|_{M_W^4} &= -1.3(7) + \frac{7}{4} \ln \frac{M_t^2}{M_W^2}, \\
A_F^{(2)} \Big|_{M_W^4} &= 0.15(5).
\end{aligned} \tag{26}$$

4.4 Results at $\mathcal{O}(\alpha_s^2)$

In this subsection we finally present the numerical corrections for $\Gamma(t \rightarrow Wb)$ at $\mathcal{O}(\alpha_s^2)$. Simply using the results derived above according to (13) and linearly adding the errors one would certainly overestimate the total uncertainty. It is more promising to add up the expansions in z for different colour structures and to perform the Padé procedure afterwards. The corresponding Padé approximations for the case $M_W = 0$ are shown in Table 9. Table 10 contains the M_W -suppressed terms. The behaviour is similar to the approach where the individual colour structures are treated separately. In the case of vanishing W boson mass the Padé results both with and without conformal mapping are highly stable. For the M_W^2 - and M_W^4 - terms, however, many of the ω -Padés develop poles inside the unit circle. The result we deduce from Tables 9 and 10 reads:

$$A^{(2)} = -16.7(8) + 5.4(4) \frac{M_W^2}{M_t^2} + \frac{M_W^4}{M_t^4} \left(11.4(5.0) - 7.3(1) \ln \frac{M_t^2}{M_W^2} \right). \tag{27}$$

The leading-order result is in very good agreement with the one of [5] which reads $-16.7(5)$. Note again that the error estimate for the M_W^4 term is rather conservative.

		$A^{(2)}$	
input	P.A.	z	ω
6	[3/2]	-16.83	-16.73
6	[2/3]	-16.84	—
7	[4/2]	-16.89	-16.49
7	[3/3]	-16.91	-15.85
7	[2/4]	-16.90	-16.79
8	[4/3]	-16.95	—
8	[3/4]	-16.95	-16.83

Table 9: Padé results for $A^{(2)}|_{M_W=0}$.

		M_W^2		M_W^4		$M_W^4 \ln(M_t^2/M_W^2)$	
input	P.A.	z	ω	z	ω	z	ω
6	[3/2]	(*) 5.774	—	—	—	-7.275	—
6	[2/3]	5.340	—	—	—	-7.281	—
7	[4/2]	5.197	—	11.54	—	-7.354	—
7	[3/3]	5.198	5.338	—	—	-7.304	—
7	[2/4]	5.280	—	11.21	—	-7.319	—

Table 10: Padé results for the coefficients of M_W^2/M_t^2 , M_W^4/M_t^4 , and $M_W^4/M_t^4 \ln M_t^2/M_W^2$ of $A^{(2)}$.

Finally we are in the position to write down the decay rate of the top quark up to order $\mathcal{O}(\alpha_s^2 M_W^4/M_t^4)$. Using the exact results at Born level and at order α_s in combination with Eq. (27) leads to:

$$\begin{aligned}
\Gamma(t \rightarrow bW) &= \Gamma_0 \left[0.8852 - 2.220 \frac{\alpha_s}{\pi} - 15.6(1.1) \left(\frac{\alpha_s}{\pi} \right)^2 + \dots \right] \\
&= 0.788(1) \Gamma_0,
\end{aligned} \tag{28}$$

where the values $M_t = 175$ GeV, $M_W = 80.4$ GeV and $\alpha_s(M_t^2) = 0.11$ have been assumed. For $M_W = 0$ the second order QCD corrections amount to roughly 2%. Both at order α_s (see Eq. (14)) and α_s^2 the M_W mass corrections “screen” the leading order terms, i.e., they arise with negative sign. Whereas the quadratic and quartic corrections at $\mathcal{O}(\alpha_s)$ turn out to be 16% and 3% w.r.t. to the massless result, they amount to roughly 7% and 1% at $\mathcal{O}(\alpha_s^2)$, respectively.

Using the $\mathcal{O}(\alpha_s^2)$ relation between M_t and the $\overline{\text{MS}}$ mass $m_t(\mu)$ [11] one may express the result in terms of $m_t \equiv m_t(m_t)$:

$$\begin{aligned}
\bar{\Gamma}(t \rightarrow bW) &= \\
&= \bar{\Gamma}_0 \left\{ 1 - 3 \frac{M_W^4}{m_t^4} + 2 \frac{M_W^6}{m_t^6} + \frac{\alpha_s}{\pi} \left[1.28 + 2 \frac{M_W^2}{m_t^2} + \frac{M_W^4}{m_t^4} \left(9.16 - 2 \ln \frac{m_t^2}{M_W^2} \right) + \dots \right] \right. \\
&\quad \left. + \left(\frac{\alpha_s}{\pi} \right)^2 \left[2.5(8) + 8.1(4) \frac{M_W^2}{m_t^2} + \frac{M_W^4}{m_t^4} \left(18.6(5.0) - 4.6(1) \ln \frac{m_t^2}{M_W^2} \right) + \dots \right] \right\} \\
&= \bar{\Gamma}_0 \left[0.8576 + 1.98 \frac{\alpha_s}{\pi} + 5.0(1.2) \left(\frac{\alpha_s}{\pi} \right)^2 + \dots \right] \\
&= 0.933(1) \bar{\Gamma}_0,
\end{aligned} \tag{29}$$

where $\bar{\Gamma}_0 = G_F m_t^3 |V_{tb}|^2 / (8\pi\sqrt{2})$, $\alpha_s(m_t^2) = 0.11$, and $m_t = 165$ GeV has been chosen. At $\mathcal{O}(\alpha_s)$ the exact result is used after the second equality sign. As expected, the convergence of the perturbative series is better in this case than in Eq. (28).

Let us finally compare the full $\mathcal{O}(\alpha_s^2)$ result with the BLM [20] contributions. They are obtained by replacing the number of light fermions in Eq. (18) by $-(\frac{33}{2} - n_l)$ and neglecting contributions from other colour factors. The result reads:

$$A^{(2),\text{BLM}} = -21.92 + 7.7(8) \frac{M_W^2}{M_t^2} + \frac{M_W^4}{M_t^4} \left(9.9(2) - \frac{161}{12} \ln \frac{M_t^2}{M_W^2} \right). \tag{30}$$

For vanishing W boson mass the difference to the complete order α_s^2 result amounts to roughly 24% and the $\mathcal{O}(M_W^2)$ term is off by almost 50%. The order of magnitude for the quartic term in M_W is reproduced correctly, but the logarithmic term differs from (27) by almost a factor of 2.

4.5 Estimate for $b \rightarrow ul\bar{\nu}$ and $\mu \rightarrow e\nu_\mu\bar{\nu}_e$

As it was pointed out in [5, 21], the results for top decay may be used to estimate also the QCD corrections to the semi-leptonic decay of the bottom quark. The $\mathcal{O}(\alpha_s^2)$ corrections to this process have been obtained recently [22] by computing four-loop on-shell diagrams. Nevertheless, using the results of the previous sections we may also derive an approximation to this quantity, in this way verifying the consistency of the results of [22], [5] and the present paper.

The decay rate for $b \rightarrow ul\bar{\nu}$ can be expressed as

$$\Gamma(b \rightarrow ul\bar{\nu}) = \Gamma_b^{(0)} + \frac{\alpha_s}{\pi} C_F \Gamma_b^{(1)} + \left(\frac{\alpha_s}{\pi} \right)^2 \Gamma_b^{(2)} + \dots \tag{31}$$

with

$$\Gamma_b^{(i)} = 2 \Gamma_b^{(0)} \int_0^1 dy A^{(i)}(y), \quad \Gamma_b^{(0)} = \frac{G_F^2 |V_{ub}|^2 M_b^5}{192\pi^3}, \tag{32}$$

where M_b is the on-shell bottom quark mass and V_{ub} is the CKM matrix element for $b \rightarrow u$ transitions. The relation to the top decay rate is established through $A^{(i)}(M_W^2/M_t^2) \equiv A^{(i)}$, with the $A^{(i)}$ defined in Eq. (13). Assuming that the functions

$$\hat{A}^{(i)}(y) \equiv \frac{A^{(i)}(y)}{A^{(0)}(y)} \quad (33)$$

are smooth within $0 < y < 1$, one may approximate them by their first few terms in the expansion around $y = 0$:

$$\hat{A}^{(i)}(y) = \sum_{n \geq 0} \left(a_n^{(i)} + a_{L,n}^{(i)} \log y \right) y^n, \quad (34)$$

which leads to

$$\Gamma_b^{(i)} = 2\Gamma_b^{(0)} \sum_{n \geq 0} \left(a_n^{(i)} \int_0^1 dy A^{(0)}(y) y^n + a_{L,n}^{(i)} \int_0^1 dy A^{(0)}(y) y^n \log y \right). \quad (35)$$

For example, in 0^{th} approximation, one finds ($a_{L,0}^{(i)} = 0$ for $i = 0, 1, 2$)

$$\Gamma_b^{(i)} = a_0^{(i)} \Gamma_b^{(0)} = A^{(i)}(0) \Gamma_b^{(0)}. \quad (36)$$

However, $\hat{A}^{(i)}(y)$ is not really smooth in general. In fact, $\hat{A}^{(1)}(y)$ has a singularity at $y = 1$ which spoils convergence of the expansion in y . On the other hand, $A^{(i)}(y) = A^{(0)}(y) \hat{A}^{(i)}(y)$ itself is finite for $y = 1$. Thus, if a larger number of terms in y is included, it is more promising to use directly Eq. (32) and expand the full integrand around small y . This is demonstrated in the case of $\Gamma_b^{(1)}$ in Table 11 where both approaches are compared including successively higher powers in y .

One can see that the approach using Eq. (35) provides reasonable estimates for $n \lesssim 4$, where, on the other hand, the results obtained by a naive expansion of the integrand in Eq. (32) are unsatisfactory. For $n > 4$, however, the situation becomes opposite: The more terms in y are included, the better is the approximation using the latter method. The method using Eq. (35) becomes very unstable.

The same procedure will now be applied at $\mathcal{O}(\alpha_s^2)$. As input we use the numbers of Eq. (27) and subtract the values for $A_l^{(2)}$ as given in Eqs. (22), (25), and (26), multiplied by $C_F T$, according to the transition from $n_l = 5$ for top decay to $n_l = 4$ for bottom decay. Only the central values from these equations will be used, the errors will be suppressed. The results are shown in Table 12. One can see that both approaches lead to results that are fairly consistent with the exact number obtained in [22].

Along the same line of reasoning we may derive an estimate for the $\mathcal{O}(\alpha^2)$ -corrections to the decay rate of the muon. Applying the obvious modifications to the notation of Eqs. (31) and (32) and using the results of Eqs. (22), (25), and (26), we find the numbers given in Table 13. Only the method according to Eq. (35) has been applied. Again these results agree nicely with the exact results obtained in [23].

This agreement can be considered as a non-trivial check of the results of [22, 23] and the ones obtained in this paper.

	$\Gamma_b^{(1)}/\Gamma_b^{(0)}$	
n	(a)	(b)
0	-2.040	-4.080
1	-1.590	-2.580
2	-2.030	-0.3333
3	-1.495	-0.9843
4	-2.093	-1.744
5	-1.327	-1.810
6	-2.371	-1.818
7	-0.8998	-1.818
8	-3.071	-1.816
9	0.2045	-1.815
10	-4.881	-1.814
exact:	-1.810	

Table 11: Estimates for $\Gamma_b^{(1)}$ using (a) Eq. (35), and (b) Eq. (32) with the full integrand replaced by its expansion around small y . n is the order of the expansion in y that was used as input.

	$\Gamma_b^{(2)}/\Gamma_b^{(0)}$	
n	(a)	(b)
0	-18.6	-37.1
1	-16.8	-31.2
2	-23.4	-24.9
exact [22]:	-21.3	

Table 12: Estimates for $\Gamma_b^{(2)}$. Same notation as in Table 11.

	$\Gamma_\mu^{(2)}/\Gamma_\mu^{(0)}$			
n	$\gamma\gamma$	elec	muon	Σ
0	3.20	2.80	-0.0636	5.94
1	2.38	2.50	-0.0343	4.85
2	4.33	3.61	-0.0397	7.90
exact [23]:	3.56	3.22	-0.0364	6.74

Table 13: Estimates for $\Gamma_\mu^{(2)}$. “ $\gamma\gamma$ ” denotes the purely photonic corrections, “elec” and “muon” the ones involving electron and muon loops, respectively. (“elec” also includes real emission of an electron-positron pair, of course.)

5 Conclusions

In this work QCD corrections of order α_s^2 to the decay of the top quark into a W boson and a bottom quark have been considered. Since the exact treatment of the contributing Feynman diagrams is currently out of question, the calculation has been reduced to the evaluation of moments. The physical limit is obtained via conformal mapping and Padé approximation. The existing results in the limit of a massless W boson could be confirmed and new terms of order M_W^2/M_t^2 and M_W^4/M_t^4 were obtained. Numerically it turns out that these power-suppressed terms are rather small. Assuming similar convergence properties concerning M_W for the one- and two-loop corrections we can conclude that the $\mathcal{O}(\alpha_s^2)$ corrections for $\Gamma(t \rightarrow Wb)$ are well under control, including finite W -mass effects.

The approach used in this article for the evaluation of the diagrams can certainly be carried over to other interesting physical problems, e.g., semileptonic bottom quark decays or muon decay as indicated in Section 4.5. In this paper the reliability of the method has been demonstrated by a comparison with a completely different approach.

Acknowledgments

We would like to thank A. Czarnecki and K. Melnikov for encouragement, numerous fruitful discussions, and providing us with a copy of [7] before its publication. We are indebted to J.H. Kühn for valuable comments, encouraging discussions, and careful reading of the manuscript. This work was supported by DFG under Contract Ku 502/8-1, the *Graduiertenkolleg "Elementarteilchenphysik an Beschleunigern"*, the *DFG-Forschergruppe "Quantenfeldtheorie, Computeralgebra und Monte-Carlo-Simulationen"* and the *Landesgraduiertenförderung* at the University of Karlsruhe, and the *Schweizer Nationalfond*.

References

- [1] J.H. Kühn, *Act. Phys. Pol.* **B 12** (1981) 374; *Act. Phys. Austr.*, Suppl. XXIV (1982) 23; I. Bigi, Y. Dokshitzer, V. Khoze, J. Kühn, and P. Zerwas, *Phys. Lett.* **B 181** (1986) 157; V.S. Fadin and V.A. Khoze, *Yad. Fiz.* **48** (1988) 487; *JETP Lett.* **46** (1987) 525.
- [2] M. Jezabek and J.H. Kühn, *Nucl. Phys.* **B 314** (1989) 1.
- [3] A. Denner and T. Sack, *Nucl. Phys.* **B 358** (1991) 46; G. Eilam, R.R. Mendel, R. Migneron, and A. Soni, *Phys. Rev. Lett.* **66** (1991) 3105.
- [4] ECFA/DESY LC Physics Working Group (E. Accomando et al.), *Phys. Reports* **299** (1998) 1.

- [5] A. Czarnecki and K. Melnikov, *Nucl. Phys. B* **544** (1999) 520.
- [6] R. Harlander and M. Steinhauser, Report Nos. BUTP-98/28, TTP98-41 (Bern, Karlsruhe, 1998), hep-ph/9812357, *Prog. Part. Nucl. Phys.* **43** (1999) 239 (in press).
- [7] A. Czarnecki and K. Melnikov, talk given at the Lake Louise Winter Institute: *Quantum Chromodynamics*, Lake Louise, Alberta, Canada, 15-21 Feb 1998. Report Nos. BNL-HET-98-22, TTP98-23 (BNL, Karlsruhe, 1998), hep-ph/9806258.
- [8] J. Fleischer and O.V. Tarasov, *Z. Phys. C* **64** (1994) 413.
- [9] D.J. Broadhurst, J. Fleischer, and O.V. Tarasov, *Z. Phys. C* **60** (1993) 287.
- [10] D.J. Broadhurst, N. Gray, and K. Schilcher, *Z. Phys. C* **52** (1991) 111.
- [11] N. Gray, D.J. Broadhurst, W. Grafe, and K. Schilcher, *Z. Phys. C* **48** (1990) 673.
- [12] A. Czarnecki, *Act. Phys. Pol. B* **26** (1995) 845.
- [13] K.G. Chetyrkin and M. Steinhauser, unpublished.
- [14] P. Nogueira, *J. Comp. Phys.* **105** (1993) 279.
- [15] Th. Seidensticker, Diploma thesis (University of Karlsruhe, 1998), unpublished.
- [16] S.A. Larin, F.V. Tkachov, and J.A.M. Vermaseren, Report No. NIKHEF-H/91-18 (Amsterdam, 1991).
- [17] M. Steinhauser, PhD thesis (University of Karlsruhe), Shaker Verlag, Aachen, 1996.
- [18] J.A.M. Vermaseren, Symbolic Manipulation with FORM, CAN (1991).
- [19] R. Harlander, T. Seidensticker, and M. Steinhauser, *Phys. Lett. B* **426** (1998) 125.
- [20] S.J. Brodsky, G.P. Lepage, and P. B. Mackenzie, *Phys. Rev. D* **28** (1983) 228.
- [21] K. Melnikov, private communication.
- [22] T. van Ritbergen, Report No. TTP99-11 (Karlsruhe, 1999), hep-ph/9903226.
- [23] T. van Ritbergen and R. Stuart, *Phys. Rev. Lett.* **82** (1999) 488; Report Nos. TTP99-18, UM-TH-99-04 (Karlsruhe, Michigan, 1999), hep-ph/9904240.